

Trimethylation of the R5 Silica-Precipitating Peptide Increases Silica Particle Size by Redirecting Orthosilicate **Binding**

Erika L. Buckle, [a] Janani Sampath, [b] Nina Michael, [a] Samuel D. Whedon, [a] Calvin J. A. Leonen, [a] Jim Pfaendtner, [b] Gary P. Drobny, [a] and Champak Chatterjee*[a]

The unmodified R5 peptide from silaffin in the diatom Cylindrotheca fusiformis rapidly precipitates silica particles from neutral aqueous solutions of orthosilicic acid. A range of posttranslational modifications found in R5 contribute toward tailoring silica morphologies in a species-specific manner. We investigated the specific effect of R5 lysine side-chain trimethylation, which adds permanent positive charges, on silica particle formation. Our studies revealed that a doubly trimethylated R5K3,4me3 peptide has reduced maximum activity yet, surprisingly, generates larger silica particles. Molecular dynamics simulations of R5K3,4me3 binding by the precursor orthosilicate anion revealed that orthosilicate preferentially associates with unmodified lysine side-chain amines and the peptide N terminus. Thus, larger silica particles arise from reduced orthosilicate association with trimethylated lysine side chains and their redirection to the N terminus of the R5 peptide.

The biological production of inorganic materials, called biomineralization, is a widespread process across the taxonomic kingdoms. Biomineralization ranges from the growth of silicates in diatoms, to calcium phosphates and carbonates in vertebrates. Silica (SiO₂) is the second most abundant biomineral on earth, and a significant proportion of silica is produced by diatoms, a type of unicellular microalgae. The cell walls (frustules) of diatoms are intricately ordered and are characterized by species-specific morphologies.^[1] These morphologies are dictated by specialized proteins referred to as silaffins. [2] Early electron microscopy efforts revealed that silica is initially deposited as nanospheres that later mature into the intricate, macroscopic structures of frustules. This suggested that silaffins may control silica sphere formation. [3] Indeed, silaffins also facilitate the production of silica particles in vitro, making them an excellent model system for studies of biosilicification. [2,4]

The soluble protein components from frustules of the marine diatom Cylindrotheca fusiformis were isolated, and their

[a] Dr. E. L. Buckle, N. Michael, Dr. S. D. Whedon, C. J. A. Leonen, Prof. Dr. G. P. Drobny, Prof. Dr. C. Chatterjee Department of Chemistry, University of Washington Seattle, WA 98195 (USA)

E-mail: chatterjee@chem.washington.edu [b] Dr. J. Sampath, Prof. Dr. J. Pfaendtner Department of Chemical Engineering, University of Washington Seattle, WA 98195 (USA)

Supporting information for this article is available on the WWW under https://doi.org/10.1002/cbic.202000264

silaffin composition elucidated. [2,5] Silaffin peptides fractionate into the components silaffin-1A_{1/2}, silaffin-1B, and silaffin-2. Silaffins 1 A_{1/2} and 1B are highly homologous, with N-terminal sequences of H-SSKKSGSYSG(S/Y) and H-SSKKSGSYYSYGT, respectively, where the underlined residues represent post-translationally modified lysines. The precursor protein Sil1p in C. fusiformis has seven repetitive silaffin sequences, sequentially labeled R1-R7. Of these, the unmodified synthetic R5 peptide co-precipitates SiO₂ similarly to the parent silaffin under ambient conditions, and has been an important model in the study of biosilicification^[4a,6] and biomineralization.^[7]

A common feature among silaffin peptides is the presence of a range of lysine post-translational modifications (PTMs).[8] These PTMs include lysine ε-amine di- and trimethylation and alkylation by oligo-N-methyl-propyleneimine units, which resemble long-chain polyamines (LCPAs). The role of isolated LCPAs in silica precipitation has been investigated with various synthetic polyamines. [9] Studies of the R5 peptide have largely focused on the role of specific amino acids by $\mathsf{NMR}^{[7b]}$ and by mutagenesis. [4a,6b] However, very little is known about the specific role of PTMs, such as trimethylation, in silica precipitation. Indeed, Lechner and Becker investigated the effect of lysine 12 trimethylation in R5 (R5K12me3) on silica morphology and activity. [6a] They observed no significant differences in the morphology of silica particles co-precipitated with either R5 or R5K12me3. However, R5K12me3 exhibited a modest increase in maximum activity over the R5 peptide. This was attributed to an increased tendency for self-assembly in phosphate buffer arising from the quaternary ammonium group. Based on our own observations that the side chains of K3 and K4 in R5, but not K12 or K15, interact closely with the SiO₂ surface, [7b] we investigated the role of trimethylation and the concomitant permanent positive charge at residues K3 and K4 in R5. A mechanistic understanding of the specific roles of trimethylation in R5 will aid future attempts to engineer novel siliceous structures and tailored materials with well-defined physical properties.

We began our studies by first synthesizing the unmodified R5 and three modified R5 peptides with trimethylation at either K3 (R5K3me3), K4 (R5K4me3) or at both residues (R5K3,4me3) (Table 1 and Figures S1 and S2).

Next, silica precipitation was undertaken at pH 7.0 with 0.2 to 3.0 mM of each peptide added to 0.1 M of silicic acid freshly generated by the hydrolysis of tetramethylorthosilicate. A modified silicomolybdate method was employed to quantify the total SiO₂ produced at each peptide concentration. ^[10] The



Table 1. Sequences of unmodified and trimethylated R5 peptides.		
Peptide	Sequence	
R5 R5K3me3 R5K4me3 R5K3,4me3	H-SSKKSGSYSGSKGSKRRIL-OH H-SSK _{me3} KSGSYSGSKGSKRRIL-OH H-SSKK _{me3} SGSYSGSKGSKRRIL-OH H-SSK _{me3} K _{me3} SGSYSGSKGSKRRIL-OH	
$K_{me3} = N^{\varepsilon}$ -trimethyl-L-lysin	e.	

data was fit to the Hill equation $[SiO_2] = [SiO_2 \text{ max}]/[1 + (EC_{50}/$ [R5]) n], where EC₅₀ is the amount of peptide required to achieve half of the maximum silica precipitated, and n is the Hill coefficient.^[7b] Interestingly, the general curve shapes and total amount of SiO₂ precipitated by each methylated variant remained similar to the unmodified R5 peptide (Figure 1 and Supplementary Information).

The maximum activity, defined as the nanomoles of silica precipitated per micromole of peptide in a fixed period of time, [6a,b] also remained similar between R5 and R5K3me3 or R5K4me3, but was significantly less for the dimethylated R5K3,4me3 peptide (Table 2).

We employed scanning electron microscopy (SEM) to evaluate changes in SiO₂ particle size and morphology upon R5 trimethylation. Elemental analysis of the particles was also

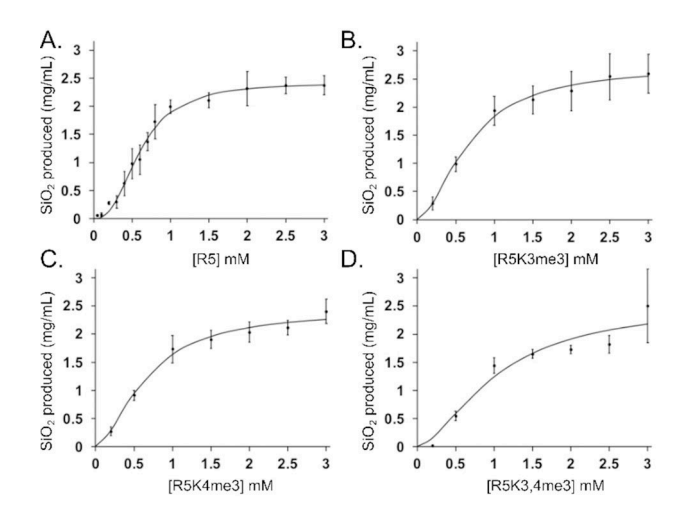


Figure 1. The effect of trimethylation on silica particle formation by R5. SiO₂ produced as a function of R5 concentration for A) unmodified R5, B) R5K3me3, C) R5K4me3, and D) R5K3,4me3. The concentration of silicic acid was held constant at 0.1 M. Silica was quantified by a modified molybdate method. n = 3, error bars show standard deviation.

Table 2. Silica-precipitating activity of R5 and its analogues.		
Peptide	Maximum activity ^[a]	Total SiO ₂ produced [μmol]
R5 R5K3me3 R5K4me3 R5K3,4me3	7.19 ± 1.26 6.49 ± 1.21 5.93 ± 1.01 4.81 ± 0.47	7.89 ± 0.57 8.63 ± 1.16 8.00 ± 0.73 8.30 ± 2.23
[a] Maximum activity measured as pmol of precipitated SiQ-/umol pentide		

in 5 min.

undertaken by energy dispersive X-ray spectroscopy (Figure S3) and all particles contained Si, O, N and C as expected for an R5-SiO₂ aggregate.^[6c] Under the conditions employed, R5 showed consistently spherical particles with an average diameter of 594 ± 93 nm (Figure 2A, B and S4). Furthermore, the Gaussian distribution envelope indicated that the resulting particles were largely uniform in size. Surprisingly, the inclusion of trimethylated lysines in R5 led to increased particle sizes in each case, with sizes of 714 \pm 95 nm for R5K3me3 (Figure 2C, D), 627 \pm 171 nm for R5K4me3 (Figure 2E, F), and 711 ± 109 nm for R5K3,4me3 (Figure 2G, H). While the particles remained spherical and followed a Gaussian size-distribution for R5K3me3 and

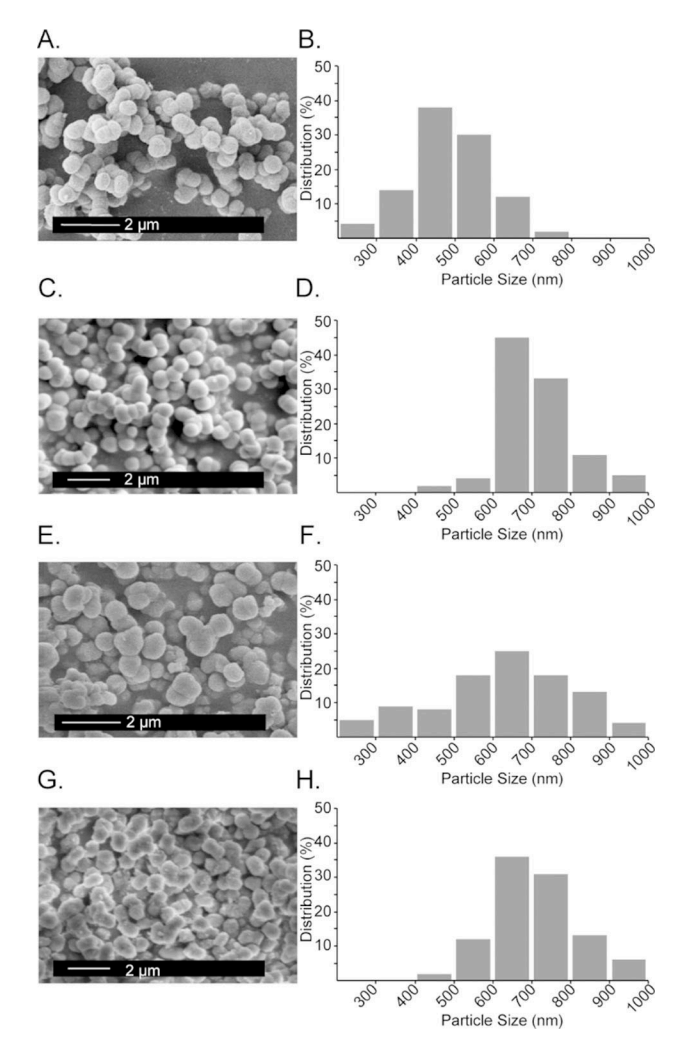


Figure 2. Scanning electron microscopy (SEM) images of SiO₂ particles generated by R5 and its trimethylated analogues. A) SEM image of SiO₂ particles co-precipitated with unmodified R5 showing spherical morphologies with a mean diameter of 594 ± 93 nm. B) Size-distribution histogram for R5-SiO₂ particles. n = 50 particles. C) SEM image of SiO₂ particles coprecipitated with R5K3me3 showing spherical morphologies with a mean diameter of 714 ± 95 nm. D) Size-distribution histogram for R5K3me3-SiO₂ particles. n = 100 particles. E) SEM image of SiO₂ particles co-precipitated with R5K4me3 showing approximately spherical morphologies with a mean diameter of 627 \pm 171 nm. F) Size-distribution histogram for R5K4me3-SiO $_{2}$ particles. n = 100 particles. G) SEM image of SiO₂ particles co-precipitated with R5K3,4me3 showing spherical morphologies with a mean diameter of 711 ± 109 nm. H) Size-distribution histogram for R5K3.4me3-SiO₂ particles. n = 100 particles. All particle sizes were measured using ImageJ.



R5K3,4me3, they were irregular and more varied in size for R5K4me3. This revealed the hitherto unknown ability of trimethylation at adjacent lysines in R5 to modify particle size and shape without changing the overall yield of precipitated silica, and also indicated the inequivalence of K3 and K4 in silica particle formation.

In order to understand nanoscale differences in peptideorthosilicate interactions underlying the observed changes in particle size and specific activity, we focused on molecular simulation. Molecular dynamics (MD) simulations in tandem with parallel bias metadynamics with partitioned families (PBMetaD-PF) was used to calculate free energy as a function of orthosilicate distance from amino groups at the N terminus and the K3/K4 side chains.[11] To facilitate using MD to study all of the relevant systems, we chose a shortened peptide corresponding to the first seven residues of R5, H-SSKKSGS-NH2, for our calculations. This is due to the fact that K3/K4 are closer to the silica surface than K12/K15, [7b] and because changes at these residues clearly influence silica morphology and specific activity (Figure 2). We note that alternative strategies to control silica morphology by modulating lysine modification state or peptide self-assembly have focused on the isolated KXXK^[12] and RRIL motifs, respectively.[13] Importantly, we found that the association of orthosilicate groups was identical in the heptamer model and full-length 19-mer R5K3me3 peptides (Figure S5).

Our calculations revealed that orthosilicate anions have a strong affinity for -NH₃⁺ at the N terminus and protonated lysine side chains (Figure 3). This was seen from the consistent energy minima at ~0.35 nm. Hence, for unmodified R5, orthosilicate binding was distributed between the N terminus and lysine side chains. For R5K3me3, however, orthosilicate anions bound the N terminus and unmethylated K4 side chain

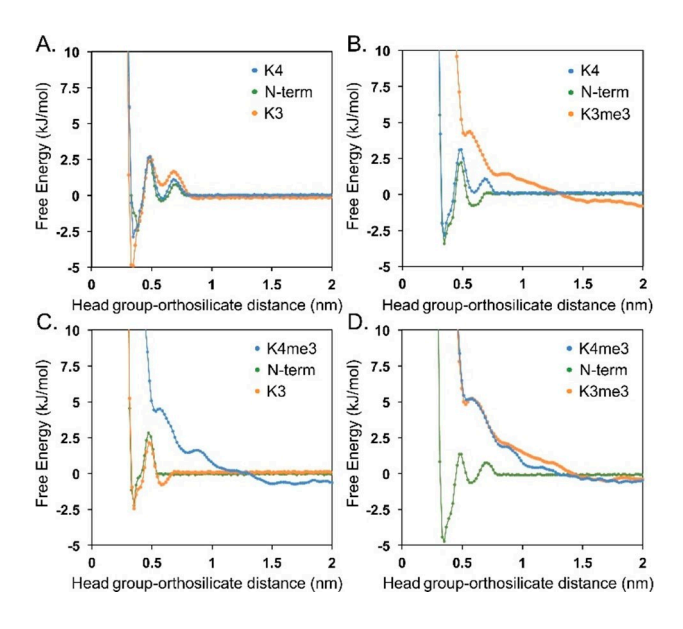


Figure 3. Computed free-energy profiles. Changes in overall free energy as a function of orthosilicate distance from the N-terminal α -amine and sidechain ε-amines for A) the unmodified R5 model peptide H-SSKKSGS-NH₂, B) the trimethylated R5 model peptide H-SSKme3KSGS-NH₂, C) the trimethylated R5 model peptide H-SSKKme3SGS-NH₂, and D) the doubly trimethylated R5 model peptide H-SSKme3Kme3SGS-NH₂.

but had no significant binding at the trimethylated K3me3 side chain (Figure 3B). Similarly, the R5K4me3 peptide bound orthosilicate at both the N terminus and K3 side chain, with no significant binding at methylated K4 (Figure 3C). Consistent with these results, the N terminus remained the only site of significant orthosilicate binding in the R5K3,4me3 peptide (Figure 3D). Orthosilicates did not effectively bind quaternary trimethylated lysine side chains at either K3 or K4, potentially due to the diffuse positive charge over three methyl groups that reduced electrostatic interactions, and the absence of strong H-bonding to the oxyanion.[14] Indeed, partial charge calculations of lysines in the heptamer peptide, with or without methylation, showed a greater dispersion of positive charge for the former (Figure 4A). Furthermore, snapshots of orthosilicate association revealed that unmethylated lysine side chains in the model R5 peptide bind orthosilicate effectively (Figure 4B). In the R5K4me3 model peptide, orthosilicate preferentially binds the unmethylated lysine residue. These results were entirely consistent with the calculated free-energy profiles (Figure 3).

The computed differences in orthosilicate association are in good agreement with the distinctly different specific activities of the R5 and R5K3,4me3 peptides (Table 2). For R5, the greater association with orthosilicate at 3 distinct amines near the peptide N terminus enhances the nucleation of silica particles, leading to a higher maximum activity. The greater degree of nucleation with R5 likely correlates with reduced particle sizes, which is consistent with previous studies of silica precipitation by short homopolymers of lysine.[15] Additionally, the lesser degree of nucleation of silica precipitation with R5K3,4me3 leads to larger particle sizes due to processes such as Ostwald ripening.[16]

In conclusion, we have performed the first investigations of trimethylation at K3 and K4 in the R5 silaffin peptide. This provides insight on chemical methods to control silica particle morphology. Trimethylation introduces a pH-insensitive positive charge at the ε-amine which may be expected to enhance

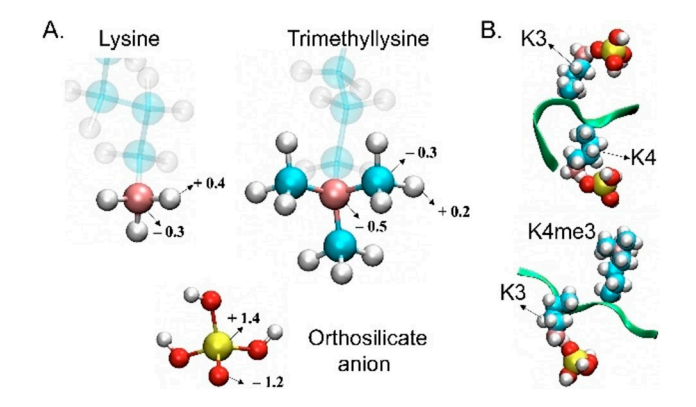


Figure 4. Calculation of partial charges in lysine side chains and their association with orthosilicate. A) Charge distribution at lysine and N^{ε} trimethyl-L-lysine amine head groups and the orthosilicate anion. Nitrogen, carbon, oxygen, silicon, and hydrogen atoms are shown in pink, blue, red, yellow, and white, respectively. B) Snapshot showing the distribution of orthosilicate anions in unmodified R5 (top) and R5K4me3 (bottom) model heptamer peptides. The peptide backbone is shown in green, and only the lysine side chains are shown as spheres.



orthosilicate binding. Surprisingly, however, we discovered that R5 specific activity decreased with increased lysine trimethylation and resulted in larger silica particles. Through atomistic MD simulations we found that orthosilicate anions do not strongly associate with trimethylated side chains, due to the diffuse positive charge over three methyl groups. The maximum amount of silica precipitated remained unchanged irrespective of the degree of R5 methylation, which indicates that silica particle size may be effectively modulated without losses in overall yields. Collectively, our results have yielded a mechanistic basis for modulating silica particle sizes and hold promise for future endeavors to engineer desired morphologies for applications in biotechnology and drug delivery. Future efforts in our labs will seek to apply our combined synthetic and computational approach toward identifying new modification combinations that control silica particle morphologies.

Acknowledgements

The authors are grateful to the Departments of Chemistry and Chemical Engineering at the University of Washington and the NSF MCB grant 1715123 and NIH 5R01GM110430 for support. Part of this work was conducted at the Molecular Analysis Facility (MAF), a National Nanotechnology Coordinated Infrastructure site at the University of Washington which is supported in part by the National Science Foundation (grant NNCI-1542101), the University of Washington, the Molecular Engineering & Sciences Institute, and the Clean Energy Institute. We also thank Scott Braswell at MAF for assistance with energy-dispersive X-ray spectroscopy and Martin Sadilek at UW Chemistry for assistance with high-resolution mass spectrometry.

Conflict of Interest

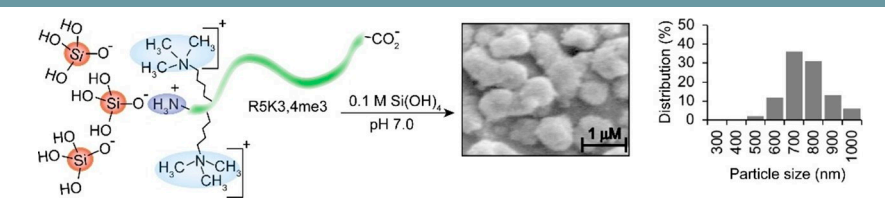
The authors declare no conflict of interest.

Keywords: particles ⋅ R5 peptide ⋅ silaffin ⋅ silica ⋅ trimethylation

- [1] N. Kroger, R. Deutzmann, C. Bergsdorf, M. Sumper, Proc. Natl. Acad. Sci. USA 2000, 97, 14133–14138.
- [2] N. Kroger, R. Deutzmann, M. Sumper, Science 1999, 286, 1129-1132.
- [3] a) B. E. Volcani, Cell Wall Formation in Diatoms: Morphogenesis and Biochemistry, Springer, New York, 1981; b) R. Gordon, R. W. Drum, Int. Rev. Cytol. 1994, 150, 243–372.
- [4] a) M. R. Knecht, D. W. Wright, Chem. Commun. 2003, 3038–3039; b) M. Sumper, N. Kroger, J. Mater. Chem. 2004, 14, 2059–2065.
- [5] N. Kroger, R. Deutzmann, M. Sumper, J. Biol. Chem. 2001, 276, 26066– 26070.
- [6] a) C. C. Lechner, C. F. W. Becker, Chem. Sci. 2012, 3, 3500–3504; b) C. C. Lechner, C. F. Becker, J. Pept. Sci. 2014, 20, 152–158; c) L. Senior, M. P. Crump, C. Williams, P. J. Booth, S. Mann, A. W. Perriman, P. Curnow, J. Mater. Chem. B 2015, 3, 2607–2614; d) K. G. Sprenger, A. Prakash, G. Drobny, J. Pfaendtner, Langmuir 2018, 34, 1199–1207.
- [7] a) S. L. Sewell, D. W. Wright, *Chem. Mater.* 2006, 18, 3108–3113; b) E. L. Buckle, A. Roehrich, B. Vandermoon, G. P. Drobny, *Langmuir* 2017, 33, 10517–10524.
- [8] C. C. Lechner, C. F. Becker, Mar. Drugs 2015, 13, 5297–5333.
- [9] a) K. M. Delak, N. Sahai, Chem. Mater. 2005, 17, 3221–3227; b) D. J. Belton, S. V. Patwardhan, C. C. Perry, J. Mater. Chem. 2005, 15, 4629–4638; c) A. Bernecker, R. Wieneke, R. Riedel, M. Seibt, A. Geyer, C. Steinem, J. Am. Chem. Soc. 2010, 132, 1023–1031.
- [10] H. W. Knudson, C. Juday, V. Meloche, Ind. Eng. Chem. Anal. Ed. 1940, 12, 270–273.
- [11] A. Prakash, C. D. Fu, M. Bonomi, J. Pfaendtner, J. Chem. Theory Comput. 2018, 14, 4985–4990.
- [12] R. Wieneke, A. Bernecker, R. Riedel, M. Sumper, C. Steinem, A. Geyer, Org. Biomol. Chem. 2011, 9, 5482–5486.
- [13] M. Kamalov, P. D. Capel, C. Rentenberger, A. R. M. Mullner, H. Peterlik, C. F. W. Becker, ChemNanoMat 2018, 4, 1209–1213.
- [14] A. N. Barrett, G. C. Roberts, A. S. Burgen, G. M. Clore, Mol. Pharmacol. 1983, 24, 443–448.
- [15] T. Coradin, O. Durupthy, J. Livage, Langmuir 2002, 18, 2331–2336.
- [16] E. Piletska, H. Yawer, F. Canfarotta, E. Moczko, K. Smolinska-Kempisty, S. S. Piletsky, A. Guerreiro, M. J. Whitcombe, S. A. Piletsky, Sci. Rep. 2017, 7, 11537.

Manuscript received: April 30, 2020
Revised manuscript received: June 27, 2020
Accepted manuscript online: June 28, 2020
Version of record online:

COMMUNICATIONS



Unexpected direction: The silaffin R5 peptide precipitates silica from solutions of orthosilicic acid. Post-translational modifications in R5 modulate silica morphology. We studied the effect of lysine trimethylation, which installs a positive

charge, on silica particle formation. Surprisingly, trimethylation led to larger particle sizes by reducing the maximum activity of R5 and redirecting orthosilicate binding to the R5N terminus.

Dr. E. L. Buckle, Dr. J. Sampath, N. Michael, Dr. S. D. Whedon, C. J. A. Leonen, Prof. Dr. J. Pfaendtner, Prof. Dr. G. P. Drobny, Prof. Dr. C. Chatterjee*

1 – 5

Trimethylation of the R5 Silica-Precipitating Peptide Increases Silica Particle Size by Redirecting Orthosilicate Binding

